Journal of Analytical and Applied Pyrolysis 171 (2023) 105937

Contents lists available at ScienceDirect

Journal of Analytical and Applied Pyrolysis

journal homepage: www.elsevier.com/locate/jaap

A thermoanalytical insight into the composition of biodegradable polymers and commercial products by EGA-MS and Py-GC-MS

Francesca De Falco [a,b,*,1], Tommaso Nacci [c,1], Lee Durndell [b], Richard C. Thompson [a], Ilaria Degano [c,d], Francesca Modugno [c,d]

[a] School of Biological and Marine Sciences, University of Plymouth, Drake Circus, PL4 8AA Plymouth, Devon, UK
[b] School of Geography, Earth and Environmental Sciences, University of Plymouth, Drake Circus, PL4 8AA Plymouth, Devon, UK
[c] Department of Chemistry and Industrial Chemistry, University of Pisa, Via G. Moruzzi 13, 56124 Pisa, Italy
[d] Center for Instrument Sharing of the University of Pisa (CISUP), University of Pisa, Italy

ARTICLE INFO

Keywords:
Biodegradable polymers
Mulch films
Fishing gears
Py-GC-MS
EGA-MS

ABSTRACT

Biodegradable polymers are proposed as a potential solution to environmental problems related to plastic pollution. Potential benefits have been suggested in applications such as agricultural mulching and fishing gear, where there can be considerable difficulty recovering products from the environment at the end of their service life. Biodegradation is a complex process influenced by both the properties of the material and the receiving environment in which it needs to biodegrade. Assessing the degradation process necessitates the chemical composition (i.e. polymer and additives) of biodegradable products to be characterised by reliable analytical methods. Pyrolysis coupled to Gas Chromatography and Mass Spectrometry (Py-GC-MS) and Evolved Gas Analysis coupled to Mass Spectrometry (EGA-MS) are emerging techniques to characterise plastic materials, providing a greater sensitivity and resolution when compared to more widely used spectroscopic techniques (FTIR and Raman). In this work, we have applied a systematic approach combining EGA-MS and multi-shot Py-GC-MS for the thermoanalytical investigation of 5 biodegradable polymers and 5 biodegradable-labelled commercial products. We identified thermal degradation profiles, main *m/z* ions and pyrolysis markers for the polymers PBAT, PBS, PBHV and two types of PLA. We applied the obtained information to investigate the composition of 4 mulch films and 1 fishing net. EGA-MS was fundamental to optimise single or multi shot pyrolysis acquisition, allowing an optimal Py-GC-MS separation and identification of the pyrolysis products. PLA and PBAT were detected in three mulch films, with the addition of starch in a film labelled as Mater-Bi and in one of unknown composition. Online silylation was crucial for detecting polysaccharides in a composite film containing hemp fibres. The presence of butylene, succinate, adipate and terephthalate units was highlighted analysing a fishing net made of a newly developed PBSAT resin. Finally, Py-GC-MS was effective in identifying the presence of additives such as 1,6-diisocyanato-hexane (chain extender) and di(3-butenyl) ester of sebacic acid derived from the plasticizer dibutyl sebacate.

1. Introduction

In recent years, biobased and biodegradable polymers have been explored as materials for a wide range of applications from biomedical to everyday use, and looked at as a potential solution to the increasing problem of plastic pollution in the environment [1–3]. The concept of "biodegradable polymers" was introduced in the literature in the 1970s, although research on biodegradable polyesters such as polyhydroxyalkanoates (PHAs) and poly(lactic acid) (PLA) dates back to the 1920s and 30s [4]. Since then, a wide range of biodegradable polymers have been developed and produced, including also poly (butylene succinate) (PBS) and poly(butylene adipate-*co*-butylene terephthalate) (PBAT).

PHAs are a class of biobased polyesters synthesized by bacteria, which includes the copolymer poly(3-hydroxybutyrate-*co*-3-hydroxyvalerate) (PHBV), characterized by good physical properties like

* Corresponding author at: School of Biological and Marine Sciences, University of Plymouth, Drake Circus, PL4 8AA Plymouth, Devon, UK.
E-mail address: francesca.defalco@plymouth.ac.uk (F. De Falco).
[1] F.D.F. and T.N. contributed equally.

https://doi.org/10.1016/j.jaap.2023.105937
Received 10 January 2023; Received in revised form 20 February 2023; Accepted 28 February 2023
Available online 1 March 2023

hardness, stability and flexibility [5].

The most studied biodegradable polymer is PLA, a thermoplastic aliphatic polyester with lactic acid as building block, produced from renewable resources [1]. Due to its chiral carbon, lactic acid has two isomers, enantiomeric *D*- and *L*- lactic acid units, which give three stereoisomeric lactide monomers: *L*-, *D*- and *meso*-lactide. The homopolymer made only of *L*-lactide is the semicrystalline poly(*L*-lactic acid) (PLLA) [6].

PBS is synthesized by polycondensation of succinic acid and 1,4-butanediol [7,8], whereas PBAT is a copolymer obtained by polycondensation between 1,4-butanediol, adipic acid, and terephthalic acid. PBAT is often used in blends with PLA and starch [9,10], a natural polysaccharide easily modified in a thermoplastic polymer and that can be blended with synthetic polymers to obtain materials like Mater-Bi [11,12].

These biodegradable polymers are often utilised in the packaging products, consumer goods, agriculture and horticulture sectors [13] and they could particularly bring advantages for products that are difficult to remove from the environment after use and that could result in formation of macro, micro or nanoplastics (e.g. agricultural mulch films, fishing gear) [14]. Agricultural mulches provide substantial benefits to crops like weed inhibition, protection from insects, increased soil temperature and minimising nutrients loss [15,16]. Biodegradable mulch films were introduced as an alternative to conventional polyethylene films, whose retrieval, recycling and landfilling was complicated and led to the generation of significant environmental pollution [17]. However, there is a lack of knowledge on the potential for environmental impacts associated with biodegradable mulch films, coupled with concerns on the effectiveness of the current international standards [14,18]. The most common synthetic polymers used in fishing gear are polyamides, which are very persistent in marine environment and once lost, these intact nets can result in ghost fishing, continuing to trap and kill marine life [19,20]. To mitigate the impact of abandoned or lost fishing nets on marine ecosystems, biodegradable polymers are object of attention and tests for this specific application [19,21,22].

In general, the polymer biodegradation process starts with a first step where the polymeric chains break down in lower molecular weight molecules (e.g. oligomers and monomers) that can be metabolized by microorganisms in a second step, ending up as biomass, carbon dioxide, methane and water [9,14]. However, different degradation mechanisms are involved, such as enzymatic or non-enzymatic hydrolysis, oxidation, photodegradation, deterioration and fragmentation [23,24]. Factors of influence include polymer characteristics like molecular weight, mechanical properties, chemical bond structure, glass transition temperature, crystallinity etc. [24–28]. The biodegradation process is also deeply influenced by the specific conditions of the environment that receives such material [14]. Exposure conditions include biotic and abiotic factors including enzymes, pH, temperature, moisture etc. [26,28,29].

The complexity of biodegradation mechanisms and the variety of factors of influence call for the development of reliable analytical methods to investigate and characterise biodegradable polymers and their lifecycle, and to follow their degradation in the environment. The first step comprises the comprehensive characterisation of the polymer matrices to establish the structural properties and features that influence the application and degradation of the material itself [30], including the presence of additives that could accelerate or hinder biodegradation [25,26]. Usually, the chemical structure of polymers is analysed by spectroscopic techniques like Fourier Transform Infrared spectroscopy (FTIR), which is widely used in degradation studies [31–34]. Recently, mass spectrometry has also been gaining significant attention and application, owing to its higher sensitivity and resolution [35], particularly when coupled with pyrolysis and gas chromatography [36,37]. Pyrolysis-Gas Chromatography-Mass Spectrometry (Py-GC-MS) is a destructive thermoanalytical techniques that has proved very effective for the identification of chemical components in polymeric materials (and other complex organic matrices), detecting minute changes in their structure, without any complicated sample pre-treatment [5,38]. Compared to other thermal techniques like thermogravimetric analysis (TGA) and differential scanning calorimetry (DSC), Py-GC-MS allows identification of thermal degradation products and therefore makes it possible reconstructing the structure and composition of the material analysed [39]. To this end, previous studies have applied Py-GC-MS to characterise biodegradable polymers including PLA [40–46], PHBV [5,47,48], PBS [45,49] and PBAT [50,51], PLA-labelled shampoo bottles [52], PLA cups and PLA/PBAT compostable plastic bags [53]. However, a systematic and thoroughly thermoanalytical investigation of biodegradable polymers with consistent Py-GC-MS methodology has yet to be conducted. Evolved Gas Analysis coupled with Mass Spectrometry (EGA-MS) and Py-GC-MS were already successfully applied to create a database of textile fibres of natural, artificial and synthetic origin, along with characteristic *m/z* ions and pyrolytic markers [54]. References exist of EGA and Py-GC-MS profiles of several polymers, but a complete database of biodegradable materials (e.g. PBAT), including possible mixtures, is lacking [55].

In this work, we apply EGA-MS and Py-GC-MS to analyse five different biodegradable polymers in the virgin pellet form (PLA, PBAT, PBS and PHBV) and five biodegradable commercial products (four mulch films and one fishing net). We aim to (1) identify thermal degradation profiles for each polymer along with main *m/z* ions and use this information to (2) select optimal temperatures to use in single or multi-shot pyrolysis; (3) identify pyrolytic markers for each polymer and (4) apply them to discriminate the chemical composition of five commercial products. It is anticipated that the data collected will inform further studies on the environmental fate of biodegradable polymers.

2. Materials and methods

2.1. Materials

The following polymers were purchased from NaturePlast® (France): poly(butylene adipate-*co*-butylene terephthalate) (PBE 006, M_n = 58,100 g/mol, M_W= 137,400 g/mol, coded as PBAT); poly(butylene succinate) (M_n = 89,800 g/mol, M_W= 188,100 g/mol, coded as PBS); poly(3-hydroxybutyrate-*co*-3-hydroxyvalerate) (PHI 003, coded as PHBV); amorphous poly(lactic acid) (PLE 005-A, M_n = 144,800 g/mol, M_W= 263,600 g/mol, coded as PLA-A); poly(*L*-lactic acid) (PLE 005, M_n =79,900 g/mol, M_W= 156,300 g/mol, coded as PLA-C). Hemp fibres were provided by East Yorkshire Hemp (UK). Four biodegradable mulch films were obtained from four different manufacturers and for anonymity were coded as MF1, MF2, MF3 and MF4. According to information supplied by the manufacturers, MF1 is a film made of PLA and PBAT, MF2 of Mater-Bi, and MF4 is a non-woven fabric mat made of PLA (95%) and hemp (5%) fibres. No information on the chemical composition of MF3 was provided. A biodegradable fishing net (coded as FG) made of poly(butylene succinate-*co*-adipate-*co*-terephthalate), PBSAT, was also examined (Table 1).

Table 1
Set of samples analysed.

Sample code	Type of product	Material composition accordingly to the manufacturer
PBAT	pellet	poly(butylene adipate-*co*-butylene terephthalate)
PBS	pellet	poly(butylene succinate)
PHBV	powder	poly(3-hydroxybutyrate-*co*-3-hydroxyvalerate)
PLA-A	pellet	amorphous poly(lactic acid)
PLA-C	pellet	poly(*L*-lactic acid)
Hemp	fibres	cellulose
MF1	mulch film	PLA/PBAT
MF2	mulch film	Mater-Bi
MF3	mulch film	unknown
MF4	mulch mat	PLA fibres with 5% hemp fibres
FG	fishing net	PBSAT

2.2. Methods

2.2.1. Evolved Gas Analysis – Mass Spectrometry (EGA-MS)

The instrumentation consisted of a Multi-Shot Pyrolyzer EGA/Py-3030D microfurnace (Frontier Laboratories Ltd. Fukushima, JP) coupled to a 6890 N Gas Chromatograph (Agilent Technologies, Palo Alto, USA). The injection port was connected to the mass spectrometer through a deactivated and uncoated stainless-steel transfer tube (UADTM-2.5 N, 0.15 mm i.d. x 2.5 m length, Frontier Lab). The gases evolved over the temperature range were transferred to the mass spectrometer, ionised, and analysed as a function of time. The detector was an Agilent 5973 Mass Selective Detector (Palo Alto, USA) single quadrupole mass spectrometer operating in electron ionisation mode (EI) at 70 eV in positive mode, scanning in the 35–600 *m/z* range. The ion source and quadrupole analyser temperatures were 230 °C and 150 °C, respectively.

70–90 μg of each sample were weighted in a clean stainless-steel cup and inserted into the microfurnace. The microfurnace was heated from 50 °C to 700 °C at 10 °C min^{-1}. The interface temperature was kept 100 °C higher than the furnace temperature up to 300 °C. The injection port operated at 280 °C with a 20:1 split ratio. The chromatographic oven was kept at 300 °C during the whole analysis. The analyses were performed in constant flow mode at 1.0 mL min^{-1} (He, purity 99.995%). The data were collected and processed by MassHunter software (version 10.0, Agilent Technologies).

Each sample was analysed in triplicate to evaluate the reproducibility of the method in terms of relative standard deviation (RSD) of peak temperature (T_P) and peak area (A_P). The T_P was calculated as the temperature corresponding to the maximum of the Total Ion Thermogram (TIT), while the A_P was obtained by dividing the area integrated from the TIT by the sample weight. The reproducibility of T_P and A_P resulted less than 2% and 8%, respectively.

2.2.2. Single and multi-shot pyrolysis – Gas Chromatography – Mass Spectrometry (Py-GC-MS)

The Py-GC-MS instrumentation consisted of a Multi-Shot Pyrolyzer EGA/Py-3030D micro-furnace (Frontier Laboratories Ltd. Fukushima, JP) coupled to an 8890 Gas Chromatograph and a 5977 Mass Selective Detector single quadrupole mass spectrometer (Agilent Technologies, Palo Alto, USA). The GC was equipped with a deactivated silica pre-column (2 m x 0.32 mm i.d., Agilent J&W, USA) and an HP-5MS fused silica capillary column (stationary phase 5% diphenyl-95% dimethylpolysiloxane, 30 m x 0.25 mm i.d., 0.25 μm, Hewlett Packard, USA).

The pyrolysis temperatures were chosen accordingly to EGA-MS results. If the thermogram showed only one thermal region, the sample was flash pyrolyzed at 600 °C, as reported in the literature for the analysis of synthetic polymers [55]. Conversely, if the thermogram featured multiple peaks, multi-shot Py-GC-MS was performed at a slightly higher temperature than the offset temperature of each band to fully characterise the pyrolysis products evolved in the whole thermal region. Thus, MF1, MF2 and MF3 samples were subjected to multi-shot Py-GC-MS, while all the other samples were pyrolyzed in single shot mode. Hemp and MF4 samples were analysed in single shot mode at 550 °C by using hexamethyldisilazane (HMDS) for the thermally assisted in-situ derivatisation of polar pyrolysis products as reported below (see Section 2.2.2.1). The specific pyrolysis conditions adopted for the analysis of each commercial product are summarized in Table 2.

For single shot analysis, around 80 μg of each sample were placed into a clean stainless-steel cup and inserted in the microfurnace through an AS-1020E Auto-Shot sampler (Frontier Laboratories Ltd., Fukushima, JP). Instead, 100–120 μg were weighted for the multi-shot analysis.

The injection port operated at 280 °C, with 30:1 split ratio, and the interface temperature was 280 °C. The pyrolysis products were eluted in constant flow mode at 1.0 mL min^{-1} (carrier gas He, purity 99.995%); the chromatographic program was: 40 °C isotherm for 6 min, 20 °C min^{-1} up to 310 °C, 310 °C isotherm for 40 min. The detector operated in electron ionisation mode (EI) at 70 eV in positive mode, scanning in the 35–550 *m/z* range. The ion source and quadrupole analyser temperatures were 230 °C and 150 °C, respectively. The collected data were processed by MassHunter Workstation (version 10.0, Agilent Technologies) and the NIST Mass Spectral Search Program (version 2.4).

Table 2
Pyrolysis conditions adopted for the Py-GC-MS analysis of the commercial products.

Sample	Pyrolysis mode	Pyrolysis temperatures
MF1	multi-shot	T_1 = 470 °C T_2 = 600 °C
MF2	multi-shot	T_1 = 340 °C T_2 = 500 °C
MF3	multi-shot	T_1 = 340 °C T_2 = 500 °C T_3 = 600 °C
MF4	single shot with HMDS	T = 550 °C
FG	single shot	T = 600 °C

Each pure reference sample was analysed in triplicate to evaluate the reproducibility of the method as the relative standard deviation (RSD) of normalised areas for selected peaks. The normalised areas were calculated by dividing the areas integrated from the Total Ion Chromatogram (TIC) by the sample weight. The peaks were selected based on their intensity and chromatographic resolution. The chosen peaks were: terephthalic acid di(3-butenyl) ester for PBAT, succinic acid 3-butenyl-4-hydroxylbutyl ester for PBS, propene for PHBV, and acetaldehyde for PLA-A and PLA-C. The reproducibility was better than 10% for all the samples.

2.2.2.1. Py(HMDS)-GC-MS. The MF4 sample and the hemp reference fibres were analysed by Py-GC-MS at 550 °C in presence of 4 μL of hexamethyldisilazane (HMDS, purity≥99%, Sigma-Aldrich, USA), exploiting in situ thermally assisted silylation to achieve superior chromatographic resolution of the polar products generated in the pyrolysis of cellulose, with the aim of enhancing the detection capability of hemp fibres in the commercial products. The instrumentation was the same one described in the previous section.

Around 100 μg of each sample were weighted for the analysis. The injection port operated at 280 °C, with 10:1 split ratio, and the interface temperature was 280 °C. The pyrolysis products were eluted in constant flow mode at 1.0 mL min^{-1} (carrier gas He, purity 99.995%); the chromatographic program was: 35 °C isotherm for 10 min, 10 °C min^{-1} up to 300 °C, 300 °C isotherm for 2 min, 20 °C min^{-1} up to 310 °C, 310 °C isotherm for 30 min. A solvent delay was applied in the first 15 min of the chromatographic run. The detector operated in electron ionisation mode (EI) at 70 eV in positive mode, scanning in the 50–600 *m/z* range. The ion source and quadrupole analyser temperatures were 230 °C and 150 °C, respectively. The collected data were processed by MassHunter Workstation (version 10.0, Agilent Technologies) and the NIST Mass Spectral Search Program (version 2.4).

3. Results and discussion

The following paragraphs will present the results obtained by EGA-MS and Py-GC-MS of pure biodegradable polymers first, and subsequently those of commercial mulch film and fishing gear samples.

3.1. Analysis of biodegradable polymers of reference

3.1.1. EGA-MS

The TITs and associated average mass spectra obtained for each type of virgin polymer and commercial product are shown in Table S1 in the Supplementary data. Starting with the virgin polymers, all TITs exhibited one main peak. The thermogram of PBAT shows a T_P = 398 °C and the average mass spectrum features signals at:

- *m/z* 44, associated with carbon dioxide, probably generated through decarboxylation reactions;
- *m/z* 54 and 55, associated with butylene;
- *m/z* 84 and 129, associated with adipic acid;
- *m/z* 105 and 149, associated with terephthalic acid;
- *m/z* 183 and 203, associated with 3-butenyl esters of adipic and terephthalic acids, respectively.

The Extract Ion Thermograms (EITs) of ions at *m/z* 55, 129 and 149 (Fig. 1) highlight the greater thermal stability of terephthalic acid compared to adipic acid. In fact, the EITs of ions at *m/z* 55 (associated with butylene) and 129 (associated with adipic acid) present a T_P of 392 °C and 396 °C, respectively, and evolve at temperatures around the T_P of the TIT peak. Instead, the EIT of ions at *m/z* 149 deriving from terephthalic acid shows a maximum at 421 °C, resulting in a broadening of the main peak of the TIT profile at temperature higher than 400 °C. This difference in the thermal behaviour of the two moieties is probably related to a stabilization induced in polyethylene glycol (PEG) polymer structure by the presence of aromatic rings.

The EGA profile of PBS features a peak at 393 °C. The average mass spectrum is dominated by signals at *m/z* 71, 101, associated with succinic acid, and 173, associated with the fragmentation of 3-butenyl ester of succinic acid. Like PBAT, two intense signals at *m/z* 54 and 55 can be observed and attributed to mass spectral features of butylene.

For PHBV, the thermal decomposition occurs in the range 250–330 °C, with a T_P = 285 °C. The average mass spectrum is dominated by the *m/z* signals at 39, 41, 45, 57, 68, 69 and 86 that can be related to the mass spectra of *Z* and *E* isomers of 2-butenoic acid, both dehydrated forms of 3-hydroxybutyric acid (HB) [55]. In fact, poly (3-hydroxybutyric acid) (PHB) generally decomposes through cis-elimination of the ester groups to form 2-butenoic acid and its oligomers [56–58]. No *m/z* signals related to pyrolysis products of poly (3-hydroxyvaleric acid) (PHV) were detected, possibly indicating a lower percentage in the sample of 3HV monomers compared to 3HB ones.

The expected different stability of semicrystalline (PLA-C) and amorphous PLA (PLA-A) is reflected in their respective thermal decomposition temperatures, equal to 367 °C and 296 °C respectively, differing by 60 °C in favour of the most thermally stable PLA-C. Fully amorphous PLA is obtained by cooling PLA to the glassy state without crystallization [59], and its structure with random and entangled chains is less resistant to thermal degradation than the organised and oriented chains of semicrystalline PLA. Regarding the corresponding average mass spectra, for PLA-A, the main ions are *m/z* 43, 45, 56 and 144, characteristic of the *meso* and *D,L*-lactides [55]. These lactide isomers are formed through intramolecular transesterification [40]. In the spectrum of PLA-C, the same main ions were detected, along with several other signals at *m/z* 72, 100 and 128, which can be related to PLA oligomers [41].

As expected, the TIT of hemp fibres features a peak at ≈ 361 °C and the associated average mass spectrum shows intense signals at *m/z* 44, 60, 69 and 73 related to the formation of anhydrosugars [54].

The analysed biodegradable polymers are all characterized by peak temperatures comprised in the range 200–400 °C, whereas the more common nonbiodegradable synthetic polymers like polyolefins, polystyrene, polyethylene terephthalate or polyamides, have all peak temperatures in the range 400–500 °C. This indicates a lower thermal stability of biodegradable polymers compared to conventional ones.

The results obtained from the analysis of the reference biodegradable polymers are summarized in Table 3, indicating the main *m/z* ions identified.

3.1.2. Py-GC-MS

Pyrograms of the analysed materials are reported in Figs. S1-S6 in the Supplementary data, along with the peak identification in Tables S2-S7. The main pyrolysis products of PBAT are 1,3-butadiene (3.5 min) and the di(3-butenyl) esters of adipic (16.9 min) and terephthalic (18.3 min) acids. The 3-butenyl ester of adipic acid and the corresponding decarboxylated form (pentanoic acid, 3-butenyl ester) are also detected at

Table 3
Characteristic *m/z* ions and pyrolysis markers of PBAT, PBS, PHBV, PLA-A, and PLA-C.

Polymer	*m/z* ions	Pyrolysis markers
PBAT	129 (adipic acid)	benzoic acid, 3-butenyl ester adipic acid, 3-butenyl ester 1,6-dioxacyclododecane-7,12-dione adipic acid, di(3-butenyl) ester terephthalic acid, di(3-butenyl) ester
	149 (terephthalic acid)	
	183 (adipic acid, di(3-butenyl) ester) 203 (terephthalic acid, di(3-butenyl) ester)	
PBS	101 (succinic acid)	succinic acid, di(3-butenyl) ester succinic acid, 3-butenyl-4-hydroxybutylester succinic acid, di(4-hydroxybuthyl) ester
	173 (succinic acid, di(3-butenyl) ester)	
PHBV	69, 86 (2-butenoic acid)	1,6,11,16-tetraoxacycloicosane-2,5,12,15-tetraone dibut-3-enyl'-butane-1,4-diyl disuccinate *(Z)*-2-butenoic acid *(E)*-2-butenoic acid
PLA	43, 56 (lactides)	3,6-dimethyl-1,4-dioxane-2,5-dion (*meso* form) 3,6-dimethyl-1,4-dioxane-2,5-dion (*DL* form)

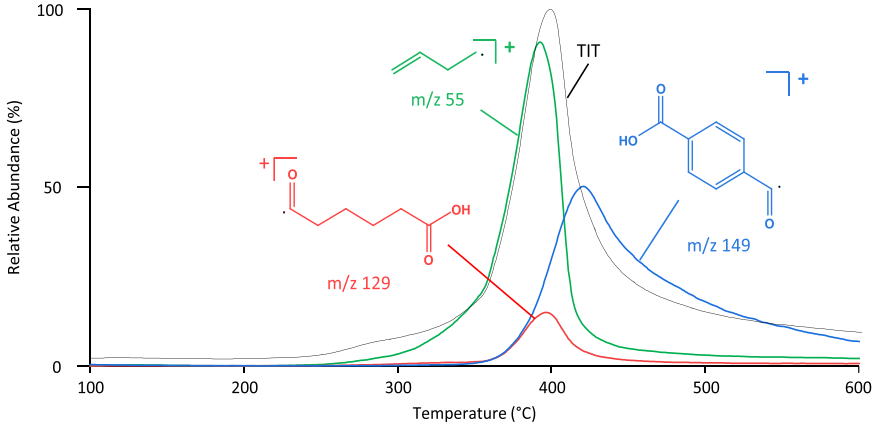

Fig. 1. TIT (black) and EITs of ions at *m/z* 55 (butylene, green), 129 (adipic acid, red), and 149 (terephthalic acid, blue) for PBAT reference sample.

15.7 and 12.5 min, respectively. The peak at 16.0 min is related to 1,6-dioxacyclododecane-7,12-dione, a lactone generated from the cyclization of adipic acid and 1,4-butanediol [60]. The pyrogram features many aromatic species such as benzene (6.1 min), benzoic acid (13.6 min), 3-butenyl ester of benzoic acid (14.7 min), biphenyl (14.9 min), and benzophenone (16.4 min) produced from the pyrolysis of the terephthalic moiety. The presence of aromatic species is confirmed by the signals at *m/z* 77, 105, and 122 in the average mass spectrum obtained from the TIT (Fig. S1). Additionally, 1,6-diisocyanato-hexane is identified at 14.7 min. This is often used as a chain extender during the polycondensation of PBAT [61-63].

The most intense peak featured in the Py-GC-MS chromatogram of PBS is related to the di(3-butenyl) ester of succinic acid (15.6 min). As for PBAT, the peak related to 1,3-butadiene is very intense, in agreement with the high relative abundance of ions at *m/z* 54 and 55 in the EGA profile. Many other derivatives of succinic acid are detected, like the 3-butenyl-4-hydroxybutyl (17.3 min) and di(4-hydroxybutyl) (19.6 min) esters, 1,6,11,16-tetraoxacycloicosane-2,5,12,15-tetraone (20.7 min), and dibut-3-enyl'-butane-1,4-diyl disuccinate (20.9 min).

The pyrolytic profile of PHBV (Fig. S1) shows the peaks at 10.2 and 11.1 min, both corresponding to 2-butenoic acid as its *Z* and *E* isomers, respectively. Some studies [5,47,48] also identified 2-pentenoic acid, a dehydrated product of 3HV, after the peaks of 2-butenoic acid. However, this compound is not detected in our pyrograms, accordingly with the EGA results.

Fig. S1 shows the pyrograms of the two forms of virgin PLA: PLA-A and PLA-C. The two materials present the same pyrolytic products, reported in Table S2. The thermal degradation of PLA involves a complex mechanism and different reactions, that lead to the formation of various compounds, and can be influenced by factors like crystallization and molecular weight distribution [64]. The peaks at 13.1 and 13.4 min correspond to the lactide isomers in the *meso* and *D,L* structures, respectively. These lactides can undergo cis-elimination and fragmentation reactions, generating acrylic acid (12.6 min) and acetaldehyde (3.5 min), respectively [40,42,44]. Ketones like 2-butanone (5.0 min) and 2,3-pentanedione (7.0 min) are also detected, possibly deriving from further fragmentation reactions. Some studies [41,43,45] identified in PLA pyrograms also larger cyclic oligomers, but our pyrograms presented no peaks after the retention time 13.4 min of the two lactide forms. This is probably due to the higher temperature of pyrolysis applied in this study compared to the literature one, leading to fragmentation of PLA oligomers.

The pyrograms of PLA-C and PLA-A differ in terms of the relative abundance of the signals corresponding to acetaldehyde and the two lactide enantiomeric forms. In PLA-C, the acetaldehyde peak is the most intense and the two peaks of the lactide forms are much smaller, whereas the opposite occurs for PLA-A. This could be explained considering the different structures of the two polymers. The greater mobility of the chains in the amorphous structure could facilitate intramolecular transesterification, leading to the formation of lactides. In the more rigid semicrystalline structure of PLA-C, radical and non-radical reactions could be energetically more favoured, producing a greater quantity of acetaldehyde. The ratio between the two lactide forms (*meso*-lactide/*D,L*-lactide) could potentially be used as a proxy to assess the biodegradation of PLA [41]. In fact, microorganisms have a preference for the *L*-lactide rather than the *D* one, causing a decrease of the intensity of the *D,L*-lactide peak in comparison to the *meso*-lactide one, following Py-GC-MS analysis [43].

The results obtained from EGA-MS and Py-GC-MS analyses of the biodegradable polymers of reference are summarized in Table 3. Recently, Okoffo et al. analysed PLA, PBAT, PBS and PHBV by reactive Py-GC-MS adding tetramethylammonium hydroxide for thermally assisted hydrolysis and methylation (TMAH) [51]. They selected and applied pyrolysis markers to detect these polymers in environmental samples. However, since their markers were all results of methylation, it is not possible to directly compare them with those resulting from our solvent and reagent-free analyses.

3.2. Analysis of commercial products

3.2.1. EGA-MS

The thermograms of the commercial products were significantly more complex than those of the reference materials, presenting one or more peaks. The thermogram of MF1 (PLA/PBAT) presents two broad thermal regions: the first one with $T_P^1 = 398$ °C, in accordance with the PBAT reference sample, and the second one with $T_P^2 = 547$ °C. The detection of ions at *m/z* 55, 129 and 203 allowed to assign the gases evolved in the first thermal region to the pyrolysis products of PBAT, whereas the average mass spectrum of the second thermal region features ions typical of aromatic species, such as *m/z* 78, 105 and 182. No *m/z* ions characteristic of PLA were detected in the average mass spectrum of MF1, probably due to its low relative abundance in the blend. PLA/PBAT blends are often used in mulch films for their excellent performance in improving crop production under different environmental conditions [65]. These two polymers are combined to overcome each other limitations. PBAT has high production costs, sensitivity to UV, low tensile strength and high melt index, characteristics that limit its processability and application as mulch film [66]. PLA is characterized by brittleness, low flexibility, low toughness and low thermal stability during processing [10,16]. By blending the two polymers, the final material shows better mechanical and thermal properties resulting in a better candidate for mulching applications [10,67].

The presence of two peaks in the TIT of MF1 could be related to the multiphase behaviour of the blend [10,68]. Kim et al. performed TGA analyses in inert atmosphere on a PLA/PBAT mulch film and also reported multiple thermal decomposition zones: 280–430 °C, 430–620 °C, and 620–780 °C [68]. The first two zones are compatible with those observed in our EGA analysis.

The TIT of MF2 (Mater-Bi) presents two peaks with different relative abundances. The first peak, at lower intensity, shows a maximum at $T_P^1 = 324$ °C and features in the associated average mass spectrum ions at *m/z* 60, 69, 73 and 98, typical of cellulose. The second thermal region is characterized by an intense peak with $T_P^2 = 404$ °C, showing in the associated average mass spectrum the typical *m/z* ions of PBAT (*m/z* 55, 129, 149, 203).

Novamont developed starch-based biodegradable materials under the Mater-Bi trademark, combining thermoplastic starch with synthetic polymers [11]. In the scientific literature, Mater-Bi mulch films are reported either as blends of starch/polycaprolactone, or of starch/PBAT [9,17,69]. Regarding our mulch film sample, EGA results suggest a composition of starch/PBAT. By incorporating the hydrophobic and mechanical properties of PBAT in the hydrophilic starch, the applicability of the material is improved [10,16].

The thermogram of MF3, a sample of unknown composition, presents a major thermal region with $T_P^2 = 400$ °C, and two smaller ones featuring $T_P^1 = 326$ °C and $T_P^3 = 550$ °C. The first small peak has an average mass spectrum with *m/z* 43, 44, 56 and 69 as most abundant ions, suggesting the presence of PLA and cellulose in the sample. The average mass spectrum associated to the main peak at 400 °C shows several main signals related to PBAT like *m/z* 39, 55, 77, 105, 129, 149 and 203. This principal peak exhibits analogous mass spectral characteristics to the peak at 404 °C of MF2, suggesting that MF3 could have a similar polymer composition, i.e. Mater-Bi. The third peak at 550 °C presents *m/z* 78, 105 and 149 as main ions in its average mass spectrum, corresponding to the same aromatic species abundant in sample MF1. The average mass spectra of the three thermal regions of observed in the TIT of sample MF3 are shown in Fig. 2.

The MF4 sample (PLA/hemp) displays a very broad peak with a maximum at 348 °C. The associated average mass spectrum shows very intense signals at *m/z* 43 and 56, corresponding to the lactide *meso* and *D,L* forms. The presence of PLA is also confirmed by the less abundant signals at *m/z* 72, 100, and 128 related to lactic acid oligomers.

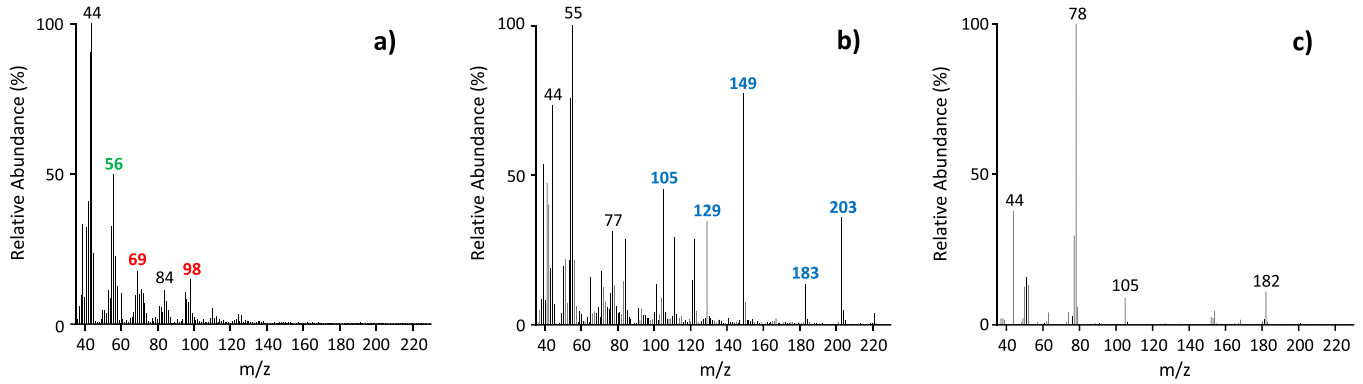

Fig. 2. Average mass spectra of a) first (258–338 °C), b) second (349–451 °C), and c) third (517–562 °C) thermal regions obtained from the TIT of sample MF3. The *m/z* ions characteristic of PLA are highlighted in green, those characteristic of cellulose in red, and those characteristic of PBAT in blue.

Unfortunately, the technique failed to detect hemp fibres, due to their low concentration in the sample.

The EGA profile of FG (PBSAT) presents a thermal region with T_P = 390 °C and a shoulder at temperatures higher than 400 °C. PBSAT was developed by combining PBS and PBAT into a single-structure copolymer at the molecular level [20]. This resin is an aliphatic-aromatic co-polyester synthesized using 1,4-butanediol, succinic acid, adipic acid and dimethyl terephthalate [70]. The ions at *m/z* 42, 55, 71, 101 and 173 account for butylene succinate in the sample, while the signals at *m/z* 129 and 203 confirm the presence of butylene adipate-*co*-terephthalate. The low intensity of *m/z* 129 and 203 ions is possibly correlated to the low percentage of the butylene adipate-*co*-terephthalate moiety in the blend.

3.3. Py-GC-MS

The commercial materials were analysed by multi-shot Py-GC-MS in conditions selected on the basis of the information on thermal features of the materials obtained from the EGA profiles.

For MF1, a first shot Py-GC-MS was performed at 470 °C and a second at 600 °C. Comparing the average mass spectra of the two thermal regions observed by EGA-MS with the mass spectra of the main chromatographic peaks observed in the TIC chromatograms of the first and second pyrolysis shots (Fig. 3), it is possible to outline a correspondence

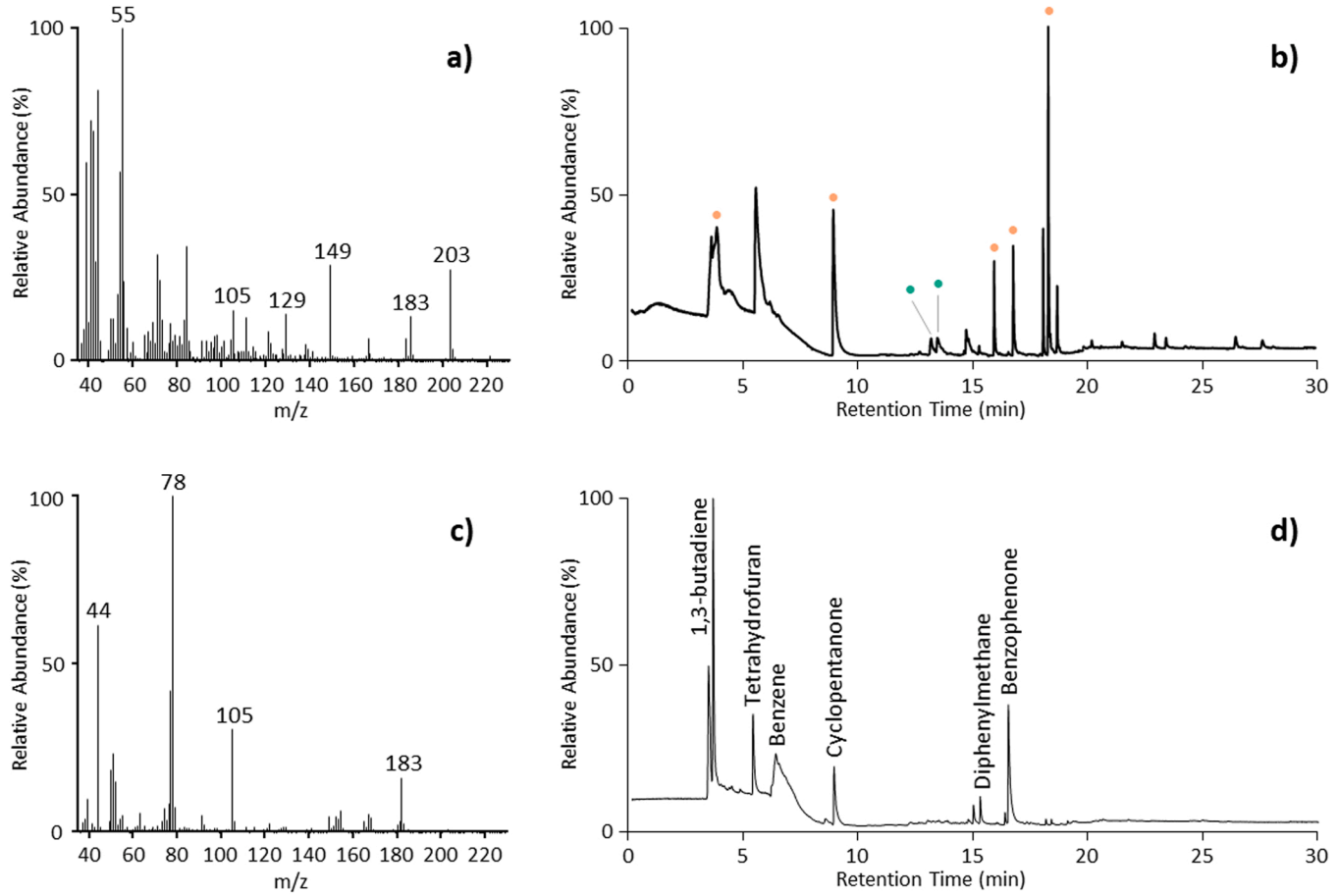

Fig. 3. a) Average mass spectrum of the first thermal region of MF1; b) first shot of MF1 (the markers of PBAT are labelled with orange dots, while those of PLA are highlighted in green); c) average mass spectrum of the second thermal region of MF1; d) second shot of MF1.

in terms of main ions and compounds identified. The average mass spectrum of the EGA-MS thermal region with $T_P^1 = 398$ °C features ions at *m/z* 55 and 84 (Fig. 3a), that are also present in the mass spectra of cyclopentanone and 1,6-dioxacyclododecane-7,12-dione, typical pyrolysis products of PBAT, found at 8.8 min and 18.1 min in the first-shot Py-GC-MS chromatogram, respectively (Fig. 3b). Moreover, the isomers of lactide are also detected in the first-shot Py-GC-MS chromatogram, at a retention time of 13.1 min for the *meso* form, and at 13.4 min for the *D,L* form (Fig. 3b). In addition, the detection of a possible product of co-pyrolysis of PBAT and PLA like 1,6-dioxacyclohexadecane-7,16-dione (18.1 min) confirms the composition of the mulch film MF1 as made of a PBAT and PLA blend. The identification of sebacic acid di(3-butenyl) ester at 18.7 min and of 1,6-diisocyanato-hexane at 14.7 min could be due to the presence of additives. In detail, di(3-butenyl) ester of sebacic acid could be a pyrolysis product derived from dibutyl sebacate, a known plasticizer added to polymeric blends to improve processability [71,72]. 1,6-diisocyanato-hexane could be a chain extender used in the synthesis of PBAT as previously reported in the list of organic additives extracted from a PBAT mulch film [62].

The Py-GC-MS chromatogram of the second shot features peaks corresponding to toluene, diphenylmethane, fluorene and triphenylmethane (Fig. 3d). The detection of aromatic species helps clarifying the origin of the intense signals at *m/z* 78 and 105 observed in the average mass spectrum related to the thermal region with $T_P^2 = 547$ °C observed in the EGA-MS thermogram (Fig. 3c). The detected species might be ascribed to reactions of hydrogenation, dehydration or benzylation of the intermediate pyrolytic products of PBAT [68]. Rizzarelli et al. already reported the presence of benzophenone in the pyrolysis products of polymer blends containing PBAT, ascribing its formation to the degradation of unidentified additives [50].

Double shot pyrolysis of MF2 was conducted at 340 °C and 500 °C. The pyrogram of the first shot at 340 °C features a peak corresponding to the lactone 1,6-dioxacyclododecane-7,12-dione (16.0 min, pyrogram in Fig. S3a), pyrolytic marker of PBAT. In addition, several pyrolysis products of unknown structure featuring *m/z* ions at 129 (23.0 min) and 149 (16.3 and 26.6 min) in their mass spectra were detected. Since 129 and 149 ions are associated with adipic and terephthalic acids, these unknown species could be co-pyrolysis products of PBAT and PLA. This hypothesis is consistent with the absence of such unknown peaks from any pyrogram of virgin material.

The second shot at 500 °C produced a chromatogram with more information about the chemical composition of MF2 with respect to the first shot (Fig. S3). Several compounds derived from PBAT are observable, the most relatively abundant being cyclopentanone and esters of adipic, phthalic and terephthalic acids. In addition, pyrolytic products characteristic of starch are also present, like pyruvic aldehyde (4.1 min), 3-buten-1-ol (5.5 min) and levoglucosan (15.8 min); as well as the *D,L*-lactide form at 13.4 min, indicating the presence of PLA. Therefore, three polymers were identified in MF2: PBAT and starch, in agreement with EGA-MS results, but also PLA that has never been documented in Mater-Bi products [9,17,69].

Regarding MF3, three thermal degradation zones were identified by EGA-MS (Fig. 2 and discussion therein); accordingly, 340, 500 and 600 °C were chosen as temperatures for the multi-shot pyrolysis experiment. The first shot pyrogram (Fig. S4a) highlights a product typical of PBAT, namely the lactone 1,6-dioxacyclododecane-7,12-dione, along with additives such as hexadecyl esters of tetradecanoic (24.2 min) and hexadecenoic (26.3 min) acids. The latter are wax esters possibly derived from the raw material used to produce cellulose [73]. The chromatogram of the second shot at 500 °C displays more peaks than that at 340 °C (a full list is provided in Table S5), leading to the identification of further PBAT pyrolytic products (cyclopentanone, 3-butenyl ester of adipic acid, monobut-3-enyl ester of phthalic acid, di(3-butenyl) ester of terephthalic acid), in addition to starch-derived compounds (pyruvic aldehyde, 1,4:3,6-dianhydro-α-D-glucopyranose) and PLA markers (3,6-dimethyl-1,4-dioxane-2,5-dion, *meso* and *D,L* forms). The pyrogram corresponding to the experiment performed at 600 °C shows peaks related to known PBAT markers such as benzene, biphenyl, 1,6-dioxacyclododecane-7,12-dione and benzophenone.

The pyrolytic products identified for MF3 are very similar to those obtained for MF2, suggesting a similar polymeric composition for the two mulch films, based on PBAT, starch and PLA. In this respect, Py-GC-MS proved to be an effective technique to identify the chemical composition of unknown commercial biodegradable products, even in the presence of mixtures. Klein et al. applied reactive Py-GC-MS (using TMAH to perform thermally assisted hydrolysis and methylation) to analyse the composition of PLA-labelled shampoo bottles, actually detecting the possible presence of pyrolysis products of different biodegradable polymers, i.e. PLA, PBS, PBSA and PBAT [52]. They performed a single shot at 600 °C and a separate thermal desorption shot at 280 °C. Differently, Capolupo et al. analysed compostable bags by single shot Py-GC-MS at 500 °C, detecting PLA and possibly PBAT [53]. In this respect, our combined approach using EGA-MS and multi-shot Py-GC-MS brings particular advantages in the analysis of polymer blends, allowing a better separation and more confident identification of the thermal decomposition products characteristic of specific polymers.

As expected, the single shot Py(HMDS)-GC-MS chromatogram of hemp fibres features peaks related to derivatised alcohols and acids, such as furfuryl alcohol (TMS), p-coumaric alcohol (2TMS), hexadecenoic and octanoic acids (TMS). The peak at 28.6 min is related to levoglucosan (3TMS), the pyrolysis marker of cellulosic fibres [74]. The pyrogram obtained from sample MF4 in the same conditions is dominated by signals related to the pyrolysis products of PLA such as lactic acid (TMS) at 19.9 min and the two lactide forms at 21.4 and 22.1 min, in agreement with EGA-MS results. However, the Extract Ion Chromatogram (EIC) of *m/z* 333 (Fig. 4), corresponding to the main fragment ion of levoglucosan (3TMS), allowed us to detect hemp fibres in the sample, confirming the higher sensitivity of Py-GC-MS compared to EGA-MS. The incorporation of natural fibres as reinforcement materials in polymer composites is indeed an increasing trend, owing to their low-cost, biodegradability, flexibility during processing, etc. [75]. Hemp fibres are often added to PLA composites to improve the mechanical strength, but the low percentage (5%) declared for MF4 is too low to generate any significant improvement in this regard [76]. An alternative explanation takes into account the addition of a natural fibre as hemp to enhance the biodegradation properties of the material.

For FG, the EGA-MS profile highlighted the presence of only one thermal degradation peak thus single shot Py-GC-MS at 600 °C was carried out. The pyrogram of sample FG (Fig. 5) shows peaks mainly related to the butylene succinate moiety such as succinic anhydride (12.3 min), di(3-butenyl) ester of succinic acid (15.6 min), 3-butenyl-4-hydroxybutyl ester of succinic acid (17.3 min), 1,6,11,16-tetraoxacycloicosane-2,5,12,15-tetraone (20.7 min) and dibut-3-enyl'-butane-1,4-diyl disuccinate (20.9 min). Moreover, 1,6-dioxacyclododecane-7,12-dione (16.0 min), di(3-butenyl) ester of adipic acid (16.9 min) and di(3-butenyl) ester of terephthalic acid (18.3 min) account for the presence of butylene adipate-*co*-terephthalate moiety. The most intense ions of the spectra of the compounds separately detected by Py-GC-MS were observed in the average mass spectra of the EGA-MS curve.

4. Conclusions

A selection of the most environmentally relevant biodegradable polymers was analysed by EGA-MS and Py-GC-MS, gathering data on their thermal degradation profiles, main *m/z* ions in the EGA-MS mass spectra, and Py-GC-MS pyrolysis markers. Previous studies have analysed biodegradable polymers, but this study represents the first comprehensive thermoanalytical investigation of such materials by combining both EGA-MS and multi-shot Py-GC-MS. EGA-MS showed that the thermal degradation profiles of PBAT, PBS, PHBV, PLA-C and PLA-A present one principal thermal region. The same reference polymers were analysed by flash (single shot) Py-GC-MS to fully characterize

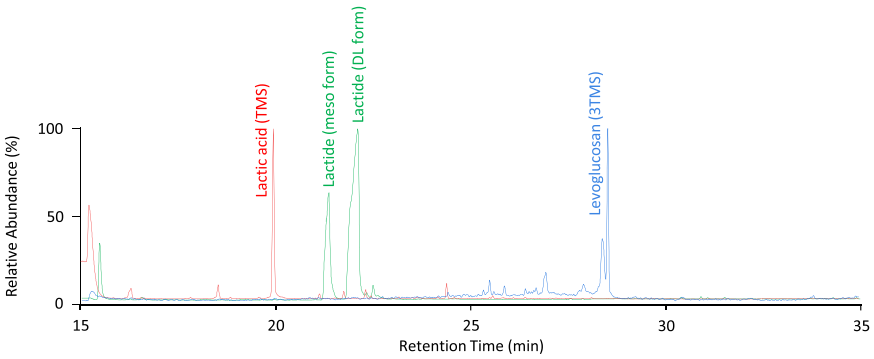

Fig. 4. Normalized EICs of ions at *m/z* 56, corresponding to lactides, *m/z* 147, corresponding to lactic acid (TMS), and *m/z* 333, corresponding to levoglucosan (3TMS), in the Py-GC-MS chromatogram of sample MF4. Identification table is reported in Table S6 in the Supplementary data.

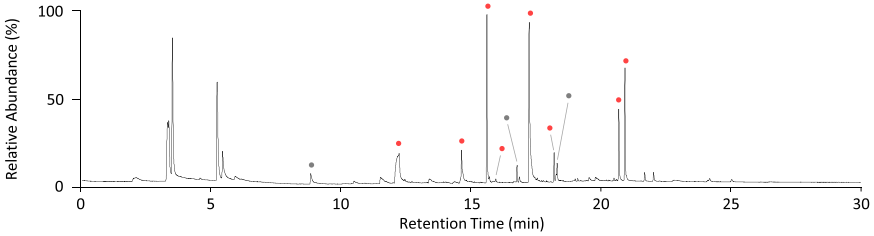

Fig. 5. Py-GC-MS chromatogram of FG sample. The markers of the butylene succinate moiety are labelled with grey dots, while those of the butylene adipate-co-terephthalate moiety are highlighted in red. Identification table is reported in Table S7 in the Supplementary data.

the related pyrolysis products. Interestingly, the EGA-MS analysis of PBAT could discriminate the different thermal stabilities of its monomers, identifying the main *m/z* ions of each moiety. Py-GC-MS analyses of both PLA (PLA-A, PLA-C) and PHBV samples identified pyrolysis markers directly related to their monomers, 3HB and lactide. The different relative intensities of the PLA pyrolysis products acetaldehyde, 3,6-dimethyl-1,4-dioxane-2,5-dion *meso* and *D,L* forms, allowed also to differentiate the thermal degradation reactions occurring for the amorphous PLA-A and the semicrystalline PLA-C. PBAT and PBS also have pyrolysis products generated from specific reactions and fragmentations of their repeating units. Therefore, the products listed in Table 2 are intrinsically related to the polymer chain composition and thus represent promising potential markers to trace the presence and degradation of these biodegradable polymers in the environment. Regarding the commercial products studied, preliminary EGA-MS analyses proved fundamental for the identification of the temperatures to be used in the following multi-shot Py-GC-MS analyses. In fact, three mulch films (MF1, MF2 and MF3) featured more than one thermal degradation zone, so double or multi shot pyrolysis was performed. The pyrolysis markers previously identified proved effective for the characterisation of the polymer composition of the commercial mulch films. The main polymer detected was PBAT, accompanied by starch and PLA. A possible co-pyrolysis product, 1,6-dioxacyclohexadecane-7,16-dione, was also identified in the PLA/PBAT blend (MF1). Both the mulch film nominally made of Mater-Bi (MF2) and that of unknown composition (MF3) were found to be composed by PBAT, PLA and starch. Silylation through the addition of HMDS in Py-GC-MS was key for the detection of cellulose pyrolysis products in the composite mulch mat made of PLA and hemp fibres (MF4). The presence of butylene, succinate, adipate and terephthalate units was also confirmed for the fishing net made of a newly developed PBSAT resin. Finally, Py-GC-MS could also identify the presence of additives in the materials analysed, such as 1,6-diisocyanato-hexane (chain extender) and di(3-butenyl) ester of sebacic acid (derived from the plasticizer dibutyl sebacate). Further experiments and analyses will be performed to apply and validate the pyrolysis markers to detect biodegradable polymers in the environment and understand their biodegradation mechanism.

Funding

The authors gratefully acknowledge the University of Pisa Visiting Fellow Programme for funding a FDF research stay at the Department of Chemistry and Industrial Chemistry in the Autumn 2021, which favoured the activation of the collaboration between the Pisa and the Plymouth groups. FDF, RCT and LD were supported by the NERC project BIO-PLASTIC-RISK (Grant NE/V007556/1).

CRediT authorship contribution statement

Francesca De Falco: Conceptualization, Methodology, Validation, Formal analysis, Data curation, Investigation, Writing – original draft. **Tommaso Nacci:** Conceptualization, Methodology, Validation, Formal analysis, Data curation, Investigation, Writing – original draft. **Lee Durndell:** Conceptualization, Visualization, Writing – review & editing. **Richard C. Thompson:** Conceptualization, Writing – review & editing, Resources, Funding acquisition. **Ilaria Degano:** Conceptualization, Methodology, Validation, Formal analysis, Resources, Writing – review & editing. **Francesca Modugno:** Conceptualization, Methodology, Formal analysis, Data curation, Writing – review & editing, Resources, Funding acquisition.

Declaration of Competing Interest

The authors declare the following financial interests/personal relationships which may be considered as potential competing interests: co-author is an Editor of JAAP - F.M.

Data Availability

All data supporting this study is provided as supplementary information accompanying this paper.

Acknowledgements

The authors acknowledge Dr. Antoine Buchard and Dr. Fannie Burgevin from the University of Bath (UK) for providing the biodegradable polymers and their molar mass information. The Centre for Instrument Sharing of the University of Pisa (CISUP) is acknowledged for providing the pyrolysis instrumentation.

Appendix A. Supporting information

Supplementary data associated with this article can be found in the online version at doi:10.1016/j.jaap.2023.105937.

References

[1] R.A. Gross, B. Kalra, Biodegradable polymers for the environment, Science (1979) vol. 297 (2002) 803–807.
[2] H. Tian, Z. Tang, X. Zhuang, X. Chen, X. Jing, Biodegradable synthetic polymers: preparation, functionalization and biomedical application, Prog. Polym. Sci. vol. 37 (2) (2012) 237–280, https://doi.org/10.1016/j.progpolymsci.2011.06.004.
[3] L. Manfra, V. Marengo, G. Libralato, M. Costantini, F. De Falco, M. Cocca, "Biodegradable polymers: a real opportunity to solve marine plastic pollution, J. Hazard Mater. vol. 416 (. 2021), https://doi.org/10.1016/j.jhazmat.2021.125763.
[4] C. Zhang, Biodegradable Polyesters: Synthesis, Properties, Applications, in: S. Fakirov (Ed.), Biodegradable Polyesters, Wiley-VCH, 2015, pp. 1–24.
[5] T.U. Khang, et al., Rapid analysis of polyhydroxyalkanoate contents and its monomer compositions by pyrolysis-gas chromatography combined with mass spectrometry (Py-GC/MS), Int. J. Biol. Macromol. vol. 174 (. 2021) 449–456, https://doi.org/10.1016/j.ijbiomac.2021.01.108.
[6] Synthesis, Structure and Properties of Poly(lactic acid), in: M.L. di Lorenzo, R. Androsch (Eds.) 279, Springer International Publishing, 2018, https://doi.org/10.1007/978–3-319–64230-7.
[7] J. Xu, B.H. Guo, Poly(butylene succinate) and its copolymers: research, development and industrialization, Biotechnol. J. vol. 5 (11) (2010) 1149–1163, https://doi.org/10.1002/biot.201000136.
[8] S.A. Rafiqah, et al., A review on properties and application of bio-based poly (Butylene succinate), Polymer vol. 13 (9) (2021), https://doi.org/10.3390/polym13091436.
[9] S. Agarwal, "Biodegradable Polymers: Present Opportunities and Challenges in Providing a Microplastic-Free Environment," Macromol Chem Phys, vol. 221, no. 6, Mar. 2020, doi: 10.1002/macp.202000017.
[10] J. Jian, Z. Xiangbin, H. Xianbo, An overview on synthesis, properties and applications of poly(butylene-adipate-co-terephthalate)–PBAT, Adv. Ind. Eng. Polym. Res. vol. 3 (1) (2020) 19–26, https://doi.org/10.1016/j.aiepr.2020.01.001.
[11] C. Bastioli, Properties and applications of Mater-Bi starch-based materials, 263–212, Polym. Degrad. Stab. vol. 59 (1998), 263–212.
[12] A. Moeini, et al., Thermoplastic starch and bioactive chitosan sub-microparticle biocomposites: antifungal and chemico-physical properties of the films, Carbohydr. Polym. vol. 230 (2020), https://doi.org/10.1016/j.carbpol.2019.115627.
[13] "Global production capacities of bioplastics 2021–2026," Nov. 2021. [Online]. Available: http://www.european-bioplastics.org/news/publications/.
[14] "Biodegradability of plastics in the open environment," Berlin, 2020. doi: 10.26356/biodegradabilityplastics.
[15] M.B.D. Tofanelli, S.E. Wortman, Benchmarking the agronomic performance of biodegradable mulches against polyethylene mulch film: a meta-analysis, Agronomy vol. 10 (10) (2020), https://doi.org/10.3390/agronomy10101618.
[16] M.A.M. Akhir, M. Mustapha, Formulation of biodegradable plastic mulch film for agriculture crop protection: a review, Polym. Rev. vol. 62 (4) (. 2022) 890–918, https://doi.org/10.1080/15583724.2022.2041031.
[17] M.B. Anunciado, et al., Effect of environmental weathering on biodegradation of biodegradable plastic mulch films under ambient soil and composting conditions, J. Polym. Environ. vol. 29 (9) (2021) 2916–2931, https://doi.org/10.1007/s10924-021-02088-4.
[18] H.Y. Sintim, M. Flury, Is biodegradable plastic mulch the solution to Agriculture's plastic problem? Environ. Sci. Technol. vol. 51 (3) (2017) 1068–1069, https://doi.org/10.1021/acs.est.6b06042.
[19] M. Deroiné, I. Pillin, G. le Maguer, M. Chauvel, Y. Grohens, Development of new generation fishing gear: A resistant and biodegradable monofilament, Polym. Test. vol. 74 (2019) 163–169, https://doi.org/10.1016/j.polymertesting.2018.11.039.
[20] K. Seonghun, K. Pyungkwan, J. Seongjae, L. Kyounghoon, Assessment of the physical characteristics and fishing performance of gillnets using biodegradable resin (PBS/PBAT and PBSAT) to reduce ghost fishing, Aquat. Conserv vol. 30 (10) (2020) 1868–1884, https://doi.org/10.1002/aqc.3354.
[21] S.W. Park, et al., Development and physical properties on the monofilament for gill nets and traps using biodegradable aliphatic polybutylene succinate resin, J. Korean Soc. Fish. Ocean Technol. vol. 43 (4) (2007) 281–290.
[22] K. Cerbule, E. Grimaldo, B. Herrmann, R.B. Larsen, J. Brčić, J. Vollstad, "Can biodegradable materials reduce plastic pollution without decreasing catch efficiency in longline fishery, Mar. Pollut. Bull. vol. 178 (2022), 113577, https://doi.org/10.1016/j.marpolbul.2022.113577.
[23] R. Chandra, Biodegradable polymers, Prog. Polym. Sci. vol. 23 (7) (1998) 1273–1335, https://doi.org/10.1016/S0079-6700(97)00039-7.
[24] N. Lucas, C. Bienaime, C. Belloy, M. Queneudec, F. Silvestre, J.E. Nava-Saucedo, Polymer biodegradation: mechanisms and estimation techniques - a review, Chemosphere vol. 73 (4) (2008) 429–442, https://doi.org/10.1016/j.chemosphere.2008.06.064.
[25] I. Kyrikou, D. Briassoulis, Biodegradation of agricultural plastic films: a critical review, J. Polym. Environ. vol. 15 (2) (. 2007) 125–150, https://doi.org/10.1007/s10924-007-0053-8.
[26] T. Kijchavengkul, R. Auras, Compostability of polymers, Polym. Int vol. 57 (6) (2008) 793–804, https://doi.org/10.1002/pi.2420.
[27] J.P. Eubeler, M. Bernhard, T.P. Knepper, Environmental biodegradation of synthetic polymers II. Biodegradation of different polymer groups, Trends Anal. Chem. vol. 29 (1) (. 2010) 84–100, https://doi.org/10.1016/j.trac.2009.09.005.
[28] B. Laycock, et al., Lifetime prediction of biodegradable polymers, Prog. Polym. Sci. vol. 71 (. 2017) 144–189, https://doi.org/10.1016/j.progpolymsci.2017.02.004.
[29] T.P. Haider, C. Völker, J. Kramm, K. Landfester, F.R. Wurm, Plastics of the Future? The impact of biodegradable polymers on the environment and on society, Angew. Chem. Int. Ed. vol. 58 (1) (. 2019) 50–62, https://doi.org/10.1002/anie.201805766.
[30] P. Rizzarelli, et al., Characterization and laser-induced degradation of a medical grade polylactide, Polym. Degrad. Stab. vol. 169 (2019), https://doi.org/10.1016/j.polymdegradstab.2019.108991.
[31] K. Pelegrini, et al., Degradation of PLA and PLA in composites with triacetin and buriti fiber after 600 days in a simulated marine environment, J. Appl. Polym. Sci. vol. 133 (15) (2016) 43290, https://doi.org/10.1002/app.43290.
[32] A. Beltrán-Sanahuja, N. Casado-Coy, L. Simó-Cabrera, C. Sanz-Lázaro, Monitoring polymer degradation under different conditions in the marine environment, Environ. Pollut. vol. 259 (. 2020), https://doi.org/10.1016/j.envpol.2019.113836.
[33] F. De Falco, et al., Comparison of biodegradable polyesters degradation behavior in sand, J. Hazard Mater. vol. 416 (2021), https://doi.org/10.1016/j.jhazmat.2021.126231.
[34] M. Niaounakis, E. Kontou, S. Pispas, M. Kafetzi, D. Giaouzi, Aging of packaging films in the marine environment, Polym. Eng. Sci. vol. 59 (s2) (2019) E432–E441, https://doi.org/10.1002/pen.25079.
[35] P. Rizzarelli, S. Carroccio, Modern mass spectrometry in the characterization and degradation of biodegradable polymers, Anal. Chim. Acta vol. 808 (2014) 18–43, https://doi.org/10.1016/j.aca.2013.11.001.
[36] R. Peñalver, N. Arroyo-Manzanares, I. López-García, M. Hernández-Córdoba, An overview of microplastics characterization by thermal analysis, Chemosphere vol. 242 (2020), 125170, https://doi.org/10.1016/j.chemosphere.2019.125170.
[37] J. la Nasa, G. Biale, D. Fabbri, F. Modugno, A review on challenges and developments of analytical pyrolysis and other thermoanalytical techniques for the quali-quantitative determination of microplastics, J. Anal. Appl. Pyrolysis vol. 149 (2020), 104841, https://doi.org/10.1016/j.jaap.2020.104841.
[38] M.P. Arrieta, J. López, S. Ferrándiz, M.A. Peltzer, Characterization of PLA-limonene blends for food packaging applications, Polym. Test. vol. 32 (4) (2013) 760–768, https://doi.org/10.1016/j.polymertesting.2013.03.016.
[39] M.P. Arrieta, F. Parres, J. López, A. Jiménez, Development of a novel pyrolysis-gas chromatography/mass spectrometry method for the analysis of poly(lactic acid) thermal degradation products, J. Anal. Appl. Pyrolysis vol. 101 (2013) 150–155, https://doi.org/10.1016/j.jaap.2013.01.017.
[40] F. Kopinke, M. Remmler, K. Mackenzie, M. Milder, Thermal decomposition of biodegradable polyesters-11. Poly(lactic acid), Polym. Degrad. Stability ! vol. 43 (1996) 329–342.
[41] F. Khabbaz, S. Karlsson, A.C. Albertsson, PY-GC/MS an effective technique to characterizing of degradation mechanism of poly (L-lactide) in the different environment, J. Appl. Polym. Sci. vol. 78 (13) (. 2000) 2369–2378, https://doi.org/10.1002/1097-4628(20001220)78:13<2369::AID-APP140>3.0.CO;2-N.
[42] C. Westphal, C. Perrot, S. Karlsson, "Py-GC/MS as a means to predict degree of degradation by giving microstructural changes modelled on LDPE and PLA," Polym Degrad Stab, vol. 73, no. 2, pp. 281–287, 2001, [Online]. Available: www.elsevier.nl/locate/polydegstab.
[43] M.P. Arrieta, E. Fortunati, F. Dominici, E. Rayón, J. López, J.M. Kenny, PLA-PHB/cellulose based films: Mechanical, barrier and disintegration properties, Polym. Degrad. Stab. vol. 107 (. 2014) 139–149, https://doi.org/10.1016/j.polymdegradstab.2014.05.010.
[44] G. Huang, et al., Thermal degradation of poly(lactide-co-propylene carbonate) measured by TG/FTIR and Py-GC/MS, Polym. Degrad. Stab. vol. 117 (2015) 16–21, https://doi.org/10.1016/j.polymdegradstab.2015.03.020.
[45] M. Llana-Ruíz-Cabello, et al., "Molecular characterisation of a bio-based active packaging containing *Origanum vulgare* L. essential oil using pyrolysis gas chromatography-mass spectrometry,", J. Sci. Food Agric. vol. 96 (9) (. 2016) 3207–3212, https://doi.org/10.1002/jsfa.7502.
[46] I. Chrysafi, N.M. Ainali, D.N. Bikiaris, Thermal Degradation Mechanism and Decomposition Kinetic Studies of Poly(Lactic Acid) and Its Copolymers with Poly (Hexylene Succinate, Polymers vol. 13 (9) (. 2021) 1365, https://doi.org/10.3390/polym13091365.
[47] M.N.F. Norrrahim, H. Ariffin, M.A. Hassan, N.A. Ibrahim, H. Nishida, Performance evaluation and chemical recyclability of a polyethylene/poly(3-hydroxybutyrate-co-3-hydroxyvalerate) blend for sustainable packaging, RSC Adv. vol. 3 (46) (2013) 24378, https://doi.org/10.1039/c3ra43632b.
[48] A. Narayanan, V.A. Sajeev Kumar, K.V. Ramana, Production and characterization of Poly (3-Hydroxybutyrate-co-3-Hydroxyvalerate) from Bacillus mycoides DFC1 using rice husk hydrolyzate, Waste Biomass-.-. Valoriz. vol. 5 (1) (2014) 109–118, https://doi.org/10.1007/s12649-013-9213-3.

[49] H. Sato et al., 2001. "A novel evaluation method for biodegradability of poly (butylene succinate-co-butylene adipate) by pyrolysis-gas chromatography," Polym Degrad Stab, vol. 73, no. 2, pp. 327–334, 2001, [Online]. Available: www.elsevier.nl/locate/polydegstab.
[50] P. Rizzarelli, et al., Determination of polyethylene in biodegradable polymer blends and in compostable carrier bags by Py-GC/MS and TGA, J. Anal. Appl. Pyrolysis vol. 117 (. 2016) 72–81, https://doi.org/10.1016/j.jaap.2015.12.014.
[51] E.D. Okoffo, C.M. Chan, C. Rauert, S. Kaserzon, K. v Thomas, Identification and quantification of micro-bioplastics in environmental samples by pyrolysis–gas chromatography–mass spectrometry, Environ. Sci. Technol. vol. 56 (19) (. 2022) 13774–13785, https://doi.org/10.1021/acs.est.2c04091.
[52] K. Klein, et al., Chemicals associated with biodegradable microplastic drive the toxicity to the freshwater oligochaete Lumbriculus variegatus, Aquat. Toxicol. vol. 231 (2021), 105723, https://doi.org/10.1016/J.AQUATOX.2020.105723.
[53] M. Capolupo, et al., Bioplastic leachates characterization and impacts on early larval stages and adult mussel cellular, biochemical and physiological responses, Environ. Pollut. vol. 319 (2023), 120951, https://doi.org/10.1016/J.ENVPOL.2022.120951.
[54] T. Nacci, F. Sabatini, C. Cirrincione, I. Degano, M.P. Colombini, Characterization of textile fibers by means of EGA-MS and Py-GC/MS, J. Anal. Appl. Pyrolysis vol. 165 (2022), 105570, https://doi.org/10.1016/j.jaap.2022.105570.
[55] J. Tsuge, H. Ohtani, C. Watanabe, 2011. Pyrolysis-GC/MS data book of synthetic polymers. Pyrograms, Thermograms and MS of Pyrolyzates., 1st ed. Oxford: Elsevier, 2011.
[56] F.D. Kopinke, M. Remmler, K. Mackenzie, Thermal decomposition of biodegradable polyesters—I: Poly(β-hydroxybutyric acid, Polym. Degrad. Stab. vol. 52 (1) (1996) 25–38, https://doi.org/10.1016/0141-3910(95)00221-9.
[57] Y. Aoyagi, K. Yamashita, Y. Doi, "Thermal degradation of poly[(R)-3-hydroxybutyrate], poly[ε-caprolactone], and poly[(S)-lactide, Polym. Degrad. Stab. vol. 76 (1) (2002) 53–59, https://doi.org/10.1016/S0141-3910(01)00265-8.
[58] H. Nishida, H. Ariffin, Y. Shirai, M. Hass, Precise depolymerization of Poly(3-hydoxybutyrate) by pyrolysis, Biopolym. Sciyo (2010), https://doi.org/10.5772/10270.
[59] E. Piorkowska, "Overview of Biobased Polymers," in Thermal Properties of Bio-based Polymers, M. L. di Lorenzo and R. Androsch, Eds. Springer, 2019, pp. 1–35. doi: 10.1007/12_2019_52.
[60] E. Canellas, P. Vera, C. Nerín, UPLC–ESI-Q-TOF-MSE and GC–MS identification and quantification of non-intentionally added substances coming from biodegradable food packaging, Anal. Bioanal. Chem. vol. 407 (22) (2015) 6781–6790, https://doi.org/10.1007/s00216-015-8848-2.
[61] J. Tuominen, J. Kylmä, J. Seppälä, Chain extending of lactic acid oligomers. 2. Increase of molecular weight with 1,6-hexamethylene diisocyanate and 2,2′-bis(2-oxazoline), Polym. (Guildf.) vol. 43 (1) (2002) 3–10, https://doi.org/10.1016/S0032-3861(01)00606-1.
[62] H. Cui, et al., Development of microwave-assisted extraction and dispersive liquid–liquid microextraction followed by gas chromatography–mass spectrometry for the determination of organic additives in biodegradable mulch films, Microchem. J. vol. 160 (. 2021), 105722, https://doi.org/10.1016/j.microc.2020.105722.
[63] K. Cai, et al., Determination of residual diisocyanates and related diamines in biodegradable mulch films using N-Ethoxycarbonylation derivatization and GC-MS, Molecules vol. 27 (19) (2022), https://doi.org/10.3390/molecules27196754.
[64] I. Chrysafi, N.M. Ainali, D.N. Bikiaris, "Thermal degradation mechanism and decomposition kinetic studies of poly(Lactic acid) and its copolymers with poly (hexylene succinate, Polym. (Basel) vol. 13 (9) (2021), https://doi.org/10.3390/polym13091365.
[65] J. Xie, et al., Prediction Model of Photodegradation for PBAT/PLA Mulch Films: strategy to fast evaluate service life, Environ. Sci. Technol. vol. 56 (12) (2022) 9041–9051, https://doi.org/10.1021/acs.est.2c01687.
[66] A.G. Souza, R.R. Ferreira, J. Harada, D.S. Rosa, Field performance on lettuce crops of poly(butylene adipate-co-terephthalate)/polylactic acid as alternative biodegradable composites mulching films, J. Appl. Polym. Sci. vol. 138 (11) (2021) 50020, https://doi.org/10.1002/app.50020.
[67] X. Gao, D. Xie, C. Yang, Effects of a PLA/PBAT biodegradable film mulch as a replacement of polyethylene film and their residues on crop and soil environment, Agric. Water Manag vol. 255 (2021), 107053, https://doi.org/10.1016/j.agwat.2021.107053.
[68] S. Kim, W. Yang, H.S. Lee, Y.F. Tsang, J. Lee, Effectiveness of CO_2-mediated pyrolysis for the treatment of biodegradable plastics: A case study of polybutylene adipate terephthalate/polylactic acid mulch film, J. Clean. Prod. vol. 372 (. 2022), 133763, https://doi.org/10.1016/j.jclepro.2022.133763.
[69] M. Menossi, M. Cisneros, V.A. Alvarez, C. Casalongué, Current and emerging biodegradable mulch films based on polysaccharide bio-composites. A review, Agron. Sustain Dev. vol. 41 (4) (. 2021) 53, https://doi.org/10.1007/s13593-021-00685-0.
[70] E. Grimaldo, et al., The effect of long-term use on the catch efficiency of biodegradable gillnets, Mar. Pollut. Bull. vol. 161 (. 2020), 111823, https://doi.org/10.1016/j.marpolbul.2020.111823.
[71] H. Liu, J. Zhang, Research progress in toughening modification of poly(lactic acid), J. Polym. Sci. B Polym. Phys. vol. 49 (15) (. 2011) 1051–1083, https://doi.org/10.1002/polb.22283.
[72] K. Buyuksoy-Fekraoui, C. Lacoste, M.F. Pucci, J.M. Lopez-Cuesta, D. Perrin, Characterization of Optimized Ternary PLA/PHB/Organoclay Composites Processed through Fused Filament Fabrication and Injection Molding, Materials vol. 15 (9) (2022) 3398, https://doi.org/10.3390/ma15093398.
[73] L.X. Zhang, Y.F. Yun, Y.Z. Liang, D.S. Cao, Discovery of mass spectral characteristics and automatic identification of wax esters from gas chromatography mass spectrometry data, J. Chromatogr. A vol. 1217 (23) (2010) 3695–3701, https://doi.org/10.1016/j.chroma.2010.03.056.
[74] S.C. Moldoveanu, Chapter 16 Pyrolysis of Carbohydrates, Tech. Instrum. Anal. Chem. vol. 28 (2010) 419–470, https://doi.org/10.1016/S0167-9244(09)02816-9.
[75] R. Siakeng, M. Jawaid, H. Ariffin, S.M. Sapuan, M. Asim, N. Saba, Natural fiber reinforced polylactic acid composites: A review, Polym. Compos vol. 40 (2) (2019) 446–463, https://doi.org/10.1002/pc.24747.
[76] G. Rajeshkumar, et al., Environment friendly, renewable and sustainable poly lactic acid (PLA) based natural fiber reinforced composites – A comprehensive review, J. Clean. Prod. vol. 310 (2021), 127483, https://doi.org/10.1016/j.jclepro.2021.127483.